

ON THE IMPORTANCE OF NUCLEAR SPIN FOR DARK MATTER DETECTION

V. A. BEDNYAKOV^{a,b}, M. A. NAZARENKO^b and F. ŠIMKOVIC^c

^a*Dzhelepov Laboratory of Nuclear Problems, Joint Institute for Nuclear Research,
141980 Dubna, Russia*

^b*Moscow State Institute of Radioengineering, Electronics and Automation
(Technical University), 78, Vernadski Avenue, 119454 Moscow, Russia*

^c*Department of Nuclear Physics, Comenius University, Mlynská dolina F1,
SK–842 15 Bratislava, Slovakia*

Received 23 October 2007; Accepted 20 February 2008
Online 18 June 2008

Weakly interacting massive particles (WIMPs) are among the main candidates for the relic dark matter (DM). The idea of the direct DM detection relies on elastic spin-dependent (SD) and spin-independent (SI) interaction of WIMPs with target nuclei. In this paper, the importance of the SD WIMP-nucleus interaction for reliable DM detection is argued. The effective low-energy minimal supersymmetric standard model (MSSM) is used for the calculation of the DM cross sections, provided the lightest neutralino is a WIMP. It is shown that the absolute lower bound for the rate of direct DM detection is due to the SD WIMP-nucleon interaction and a new-generation experiment aimed at *detecting* DM with sensitivity higher than 10^{-5} event/day/kg should have a non-zero-spin target to avoid missing of the DM signal.

PACS numbers: 95.35.+d, 12.60.Jv, 14.80.Ly

UDC 539.12

Keywords: dark matter, weakly interacting massive particle, supersymmetry, neutralino, nuclear spin matrix element

1. Introduction

Galactic dark matter (DM) particles do not emit any electromagnetic radiation and only gravitationally manifest themselves affecting other, visible, astrophysical objects. Historically, the first evidence of this kind came from the study of galactic rotation curves, when one measures the velocity with which globular stellar clusters, gas clouds, or dwarf galaxies orbit around their centers. If the mass of these galaxies were concentrated in their visible parts, the orbital velocity at large radii r should decrease in accordance with Kepler's law as $1/\sqrt{r}$. Instead, it remains ap-

proximately constant to the largest radius where it can be measured. This implies that the total mass $M(r)$ felt by an object at a radius r must increase linearly with r . Studies of this type imply that 90% or more of the mass of large galaxies is dark.

The mass density averaged over the entire Universe is usually expressed in units of critical the density $\rho_c \approx 10^{-29} \text{g/cm}^3$, the dimensionless ratio $\Omega \equiv \rho/\rho_c = 1$ corresponds to a flat Universe. Studies of clusters and superclusters of galaxies through gravitational lensing or through measurements of their X-ray temperature, as well as studies of the large-scale streaming of galaxies favor larger values of the total mass density of the Universe $\Omega \geq 0.3$ (see, for example Ref. [1]).

Exciting evidence for a flat and accelerating universe was obtained [2, 3]. The position of the first acoustic peak of the angular power spectrum (of temperature anisotropy of cosmic microwave background radiation) strongly suggests a flat universe with density parameter $\Omega_0 = 1$, while the shape of the peak is consistent with the density perturbations predicted by models of inflation. Data support $\Omega_0 = \Omega_M + \Omega_\Lambda = 1$ where Ω_M is the matter density in the Universe and Ω_Λ is the contribution of the non-zero cosmological constant (the energy density of the vacuum). Recent Wilkinson Microwave Anisotropy Probe (WMAP) investigations [4, 5] of the cosmic microwave background and measurements of its temperature anisotropy supplied us with most precise values for the cosmological parameters (Table 1). The parameters unambiguously confirm the existence of large amount of the dark matter. Most DM must therefore be non-baryonic. “New physics” beyond the the Standard Model of particle physics is required to describe this exotic matter. We omit discussion of the dark energy — another mysterious substance in the Universe, which fill the gap between flat Universe and measured amount of dark matter ($\Omega_{\text{DM}} + \Omega_{\text{DE}} = \Omega_{\text{total}} = 1$). In 2007, a very exiting “visualization” of the invisible DM substance (Fig. 1) has been obtained by mean of gravitation lensing [6]. The local density of DM amounts to about $\rho_{\text{local}}^{\text{DM}} \simeq 0.3 \text{ GeV/cm}^3 \simeq 5 \cdot 10^{-25} \text{g/cm}^3$. It is assumed to have a Maxwellian velocity distribution with mean $\bar{v} \simeq 300 \text{ km/s}$. The local flux of DM particles χ is $\Phi_{\text{local}}^{\text{DM}} \simeq \frac{100 \text{ GeV}}{m_\chi} \cdot 10^5 \text{ cm}^{-2}\text{s}^{-1}$. This respectable value is considered as the basis for direct search for DM particles.

Weakly interacting massive particles (WIMPs) are among the most popular candidates for the relic DM. The lightest supersymmetric (SUSY) particle (LSP), neutralino, is assumed to be the best WIMP DM candidate. The main efforts and

TABLE 1. Some basic cosmological parameters from WMAP [4, 5].

Hubble constant	$h = 0.71^{+0.04}_{-0.03}$
Baryon density	$\Omega_b h^2 = 0.0224 \pm 0.0009$
Matter density	$\Omega_M h^2 = 0.135^{+0.008}_{-0.009}$
Baryon/critical density	$\Omega_b = 0.044 \pm 0.004$
Matter/critical density	$\Omega_M = 0.27 \pm 0.04$
Total/critical density	$\Omega_{\text{tot}} = 1.02 \pm 0.02$

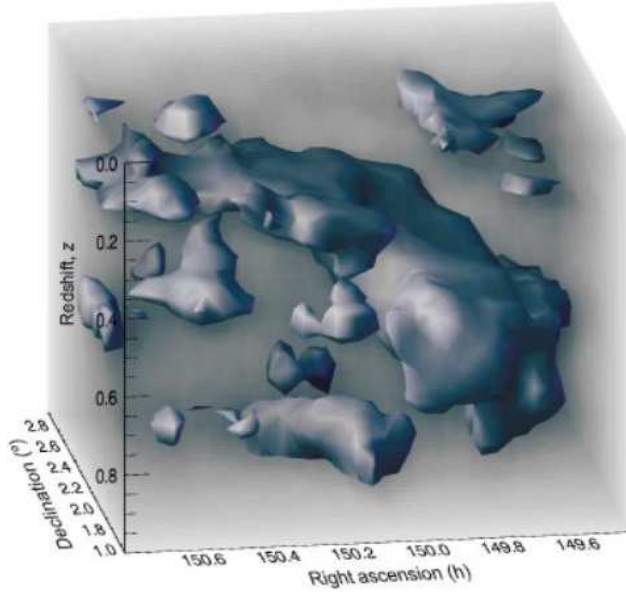


Fig. 1. Three-dimensional reconstruction of the dark matter distribution. From Ref. [6].

expectations in the direct DM searches are concentrated in the field of the so-called spin-independent (or scalar) interaction of a DM WIMP with a target nucleus. It is believed that for heavy enough nuclei this spin-independent (SI) interaction of DM particles with nuclei usually gives the dominant contribution to the expected event rate of its detection. The reason is the strong (proportional to the squared mass of the target nucleus) enhancement of SI WIMP-nucleus interaction. The results obtained in the field are presented in the form of exclusion curves (Fig. 2). For a fixed mass of the WIMP, the cross sections of SI elastic WIMP-nucleon inter-

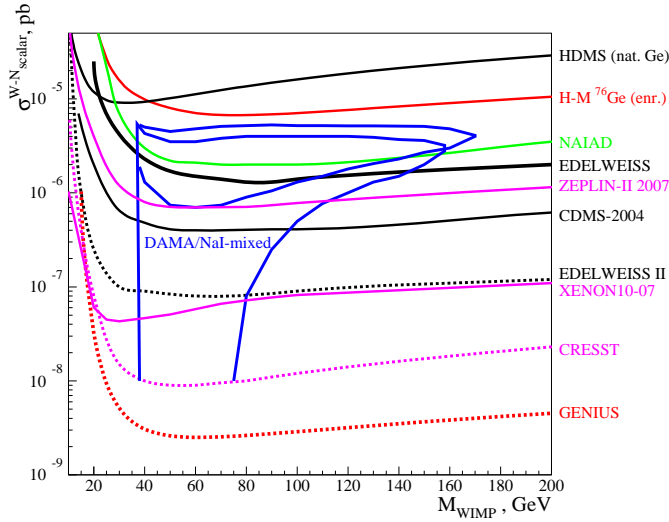


Fig. 2. WIMP-nucleon cross section limits for scalar (SI) interactions as a function of the WIMP mass. The closed DAMA/NaI contour corresponds to a complete neglect of spin-dependent WIMP-nucleon interaction ($\sigma_{SD} = 0$), while the open contour is obtained with the assumption that $\sigma_{SD} = 0.08$ pb [8]. From Ref. [10].

action located above these curves are excluded.

Only the DAMA collaboration claims observation of the first evidence for the dark matter signal, due to registration of the annual modulation effect [7, 9]. The main result of the DAMA observation of the annual modulation signature is the low-mass region of the WIMPs ($40 < m_\chi < 150$ GeV) and relatively high allowed SI or/and SD cross sections, provided these WIMPs are cold dark matter particles. It is obvious that such a serious claim should be verified at least by one other completely independent experiment. To confirm this DAMA result, one should perform a new experiment which would have the same or better sensitivity to the annual modulation signal in a reasonable time. The spin-1/2 weakly-interacting massive particles were considered as the first cold DM candidates. They interact with ordinary matter predominantly by means of axial vector (spin-dependent) and vector (spin-independent) couplings. In 1994 it was claimed in Ref. [11] that nuclear spin is not important for detection of the dark matter particles, provided the detection sensitivity does not exceed 0.01 events/day/kg, which was considered unreachable at that time. Now the situation has changed and we would like to notice that for targets with spin-non-zero nuclei, it might be the spin-dependent interaction that determines the lower bound for the direct detection rate when the cross section of the scalar interaction, which is usually assumed to be the dominant part, drops below $10^{-12 \div 13}$ pb [12].

2. Event rate and cross sections

One believes to detect directly a relic DM WIMP with mass m_χ via its elastic scattering on a target nucleus (A, Z). The nuclear recoil energy E_R is measured by a proper detector deeply underground (Fig. 3). The differential event rate in respect

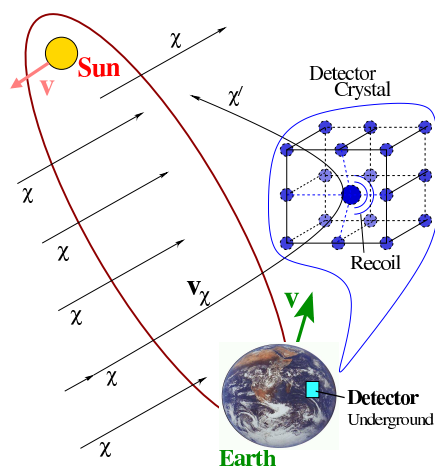


Fig. 3. Due to the expected annual modulation signature of the event rate (1), only the Sun-Earth system is a proper setup for the successful direct DM detection.

to the recoil energy is the subject of experimental measurements. The rate depends on the velocity distribution of the relic WIMPs in the solar vicinity $f(v)$ and the cross section of WIMP-nucleus elastic scattering [13–19, 11]. The differential event rate per unit mass of the target material has the form

$$\frac{dR}{dE_R} = N_T \frac{\rho_\chi}{m_\chi} \int_{v_{\min}}^{v_{\max}} dv f(v) v \frac{d\sigma^A(v, q^2)}{dq^2}. \quad (1)$$

We assume these WIMPs to be a dominant component of the DM halo of our Galaxy with a density $\rho_\chi = 0.3 \text{ GeV/cm}^3$. The nuclear recoil energy $E_R = q^2/(2M_A)$ is typically about $10^{-6}m_\chi$ and N_T is the number density of target nuclei with mass M_A . $v_{\max} = v_{\text{esc}} \approx 600 \text{ km/s}$, $v_{\min} = (M_A E_R/2\mu_A^2)^{1/2}$. The WIMP-nucleus differential elastic scattering cross section for spin-non-zero ($J \neq 0$) nuclei contains coherent (spin-independent, or SI) and axial (spin-dependent, or SD) terms [21, 20, 22]

$$\frac{d\sigma^A(v, q^2)}{dq^2} = \frac{\sigma_{\text{SD}}^A(0)}{4\mu_A^2 v^2} F_{\text{SD}}^2(q^2) + \frac{\sigma_{\text{SI}}^A(0)}{4\mu_A^2 v^2} F_{\text{SI}}^2(q^2). \quad (2)$$

The normalized ($F_{\text{SD,SI}}^2(0) = 1$) finite-momentum-transfer nuclear form-factors $F_{\text{SD,SI}}^2(q^2)$ can be expressed through the nuclear structure functions [21, 20, 22–24]. For $q = 0$ the nuclear SD and SI cross sections can be presented as follows

$$\sigma_{\text{SI}}^A(0) = \frac{4\mu_A^2 S_{\text{SI}}(0)}{(2J+1)} = \frac{\mu_A^2}{\mu_p^2} A^2 \sigma_{\text{SI}}^p(0), \quad (3)$$

$$\sigma_{\text{SD}}^A(0) = \frac{4\mu_A^2 S_{\text{SD}}(0)}{(2J+1)} = \frac{4\mu_A^2 (J+1)}{\pi J} \{a_p \langle \mathbf{S}_p^A \rangle + a_n \langle \mathbf{S}_n^A \rangle\}^2 \quad (4)$$

$$= \frac{\mu_A^2}{\mu_p^2} \frac{4}{3} \frac{J+1}{J} \sigma_{\text{SD}}^{pn}(0) \{ \langle \mathbf{S}_p^A \rangle \cos \theta + \langle \mathbf{S}_n^A \rangle \sin \theta \}^2. \quad (5)$$

Following Bernabei et al. [8, 25], the effective spin WIMP-nucleon cross section $\sigma_{\text{SD}}^{pn}(0)$ and the coupling mixing angle θ were introduced

$$\sigma_{\text{SD}}^{pn}(0) = \frac{\mu_p^2}{\pi} \frac{4}{3} [a_p^2 + a_n^2], \quad \tan \theta = \frac{a_n}{a_p}; \quad (6)$$

$$\sigma_{\text{SD}}^p = \sigma_{\text{SD}}^{pn} \cdot \cos^2 \theta, \quad \sigma_{\text{SD}}^n = \sigma_{\text{SD}}^{pn} \cdot \sin^2 \theta. \quad (7)$$

Here, $\mu_A = \frac{m_\chi M_A}{m_\chi + M_A}$ is the reduced mass of the neutralino and the nucleus and it is assumed that $\mu_n^2 = \mu_p^2$. The dependence on effective WIMP-quark (in SUSY neutralino-quark) couplings \mathcal{C}_q and \mathcal{A}_q in the underlying theory

$$\mathcal{L}_{\text{eff}} = \sum_q (\mathcal{A}_q \cdot \bar{\chi} \gamma_\mu \gamma_5 \chi \cdot \bar{q} \gamma^\mu \gamma_5 q + \mathcal{C}_q \cdot \bar{\chi} \chi \cdot \bar{q} q) + \dots \quad (8)$$

and on the spin ($\Delta_q^{(p,n)}$) and the mass ($f_q^{(p)} \approx f_q^{(n)}$) structure of the proton and neutron enter into these equations via WIMP-proton and WIMP-neutron SI and SD cross sections at $q = 0$:

$$\sigma_{\text{SI}}^p(0) = 4 \frac{\mu_p^2}{\pi} c_0^2, \quad c_0 = c_0^{p,n} = \sum_q \mathcal{C}_q f_q^{(p,n)}, \quad (9)$$

$$\sigma_{\text{SD}}^{p,n}(0) = 12 \frac{\mu_{p,n}^2}{\pi} a_{p,n}^2, \quad a_p = \sum_q \mathcal{A}_q \Delta_q^{(p)}, \quad a_n = \sum_q \mathcal{A}_q \Delta_q^{(n)}. \quad (10)$$

The factors $\Delta_q^{(p,n)}$, which parameterize the quark spin content of the nucleon, are defined as $2\Delta_q^{(n,p)} s^\mu \equiv \langle p, s | \psi_q \gamma^\mu \gamma_5 \psi_q | p, s \rangle_{(p,n)}$. The $\langle \mathbf{S}_{p(n)}^A \rangle$ is the total spin of protons (neutrons) averaged over all A nucleons of the nucleus (A, Z): $\langle \mathbf{S}_{p(n)}^A \rangle \equiv \langle A | \mathbf{S}_{p(n)}^A | A \rangle = \langle A | \sum_i^A \mathbf{s}_{p(n)}^i | A \rangle$. The mean velocity $\langle v \rangle$ of the relic neutralinos of our Galaxy is about $300 \text{ km/s} = 10^{-3}c$. Assuming $q_{\text{max}}R \ll 1$, where R is the nuclear radius and $q_{\text{max}} = 2\mu_A v$ is the maximum of the momentum transfer in the process of the χA scattering, the SD matrix element takes a simple form (*zero momentum transfer limit*) [26, 27]

$$\mathcal{M} = C \langle A | a_p \mathbf{S}_p + a_n \mathbf{S}_n | A \rangle \cdot \mathbf{s}_\chi = C \Lambda \langle A | \mathbf{J} | A \rangle \cdot \mathbf{s}_\chi. \quad (11)$$

Here, \mathbf{s}_χ denotes the spin of the neutralino, and

$$\Lambda = \frac{\langle N | a_p \mathbf{S}_p + a_n \mathbf{S}_n | N \rangle}{\langle N | \mathbf{J} | N \rangle} = \frac{\langle N | (a_p \mathbf{S}_p + a_n \mathbf{S}_n) \cdot \mathbf{J} | N \rangle}{J(J+1)} = \frac{a_p \langle \mathbf{S}_p \rangle}{J} + \frac{a_n \langle \mathbf{S}_n \rangle}{J}. \quad (12)$$

Note a coupling of the spin of χ to the spin carried by the protons and the neutrons. The uncertainties arising from the electroweak and QCD scale physics are incorporated in the factors a_p and a_n . For the most interesting isotopes, either $\langle \mathbf{S}_p^A \rangle$ or $\langle \mathbf{S}_n^A \rangle$ dominates ($\langle \mathbf{S}_{n(p)}^A \rangle \ll \langle \mathbf{S}_{p(n)}^A \rangle$). See, for example, Table 2.

The differential event rate (1) can be given also in the form [8, 10]:

$$\begin{aligned} \frac{dR(E_R)}{dE_R} &= \kappa_{\text{SI}}(E_R, m_\chi) \sigma_{\text{SI}} + \kappa_{\text{SD}}(E_R, m_\chi) \sigma_{\text{SD}}. \quad (13) \\ \kappa_{\text{SI}}(E_R, m_\chi) &= N_T \frac{\rho_\chi M_A}{2m_\chi \mu_p^2} B_{\text{SI}}(E_R) [M_A^2], \\ \kappa_{\text{SD}}(E_R, m_\chi) &= N_T \frac{\rho_\chi M_A}{2m_\chi \mu_p^2} B_{\text{SD}}(E_R) \left[\frac{4}{3} \frac{J+1}{J} (\langle \mathbf{S}_p \rangle \cos \theta + \langle \mathbf{S}_n \rangle \sin \theta)^2 \right], \quad (14) \\ B_{\text{SI,SD}}(E_R) &= \frac{\langle v \rangle}{\langle v^2 \rangle} F_{\text{SI,SD}}^2(E_R) I(E_R). \end{aligned}$$

TABLE 2. Zero momentum spin structure of nuclei in different models. The measured magnetic moments used as input are enclosed in parentheses. From Ref. [23].

$^{73}\text{Ge} (L_J = G_{9/2})$			
	$\langle \mathbf{S}_p \rangle$	$\langle \mathbf{S}_n \rangle$	μ (in μ_N)
ISPSM, Ellis–Flores [28, 29]	0	0.5	−1.913
OGM, Engel–Vogel [30]	0	0.23	(−0.879) _{exp}
IBFM, Iachello et al. [31, 22]	−0.009	0.469	−1.785
IBFM (quenched), Iachello et al. [31, 22]	−0.005	0.245	(−0.879) _{exp}
TFFS, Nikolaev–Klapdor-Kleingrothaus [32]	0	0.34	—
SM (small), Ressel et al. [22]	0.005	0.496	−1.468
SM (large), Ressel et al. [22]	0.011	0.468	−1.239
SM (large, quenched), Ressel et al. [22]	0.009	0.372	(−0.879) _{exp}
“Hybrid” SM, Dimitrov et al. [33]	0.030	0.378	−0.920
$^{127}\text{I} (L_J = D_{5/2})$			
ISPSM, Ellis–Flores [29, 34]	1/2	0	4.793
OGM, Engel–Vogel [30]	0.07	0	(2.813) _{exp}
IBFM, Iachello et al. [31]	0.464	0.010	(2.813) _{exp}
IBFM (quenched), Iachello et al. [31]	0.154	0.003	(2.813) _{exp}
TFFS, Nikolaev–Klapdor-Kleingrothaus [32]	0.15	0	—
SM (Bonn A), Ressel–Dean [27]	0.309	0.075	2.775 {2.470} _{eff}
SM (Nijmegen II), Ressel–Dean [27]	0.354	0.064	3.150 {2.7930} _{eff}
$^{131}\text{Xe} (L_J = D_{3/2})$			
ISPSM, Ellis–Flores [28, 29]	0	−0.3	1.148
OGM, Engel–Vogel [30]	0.0	−0.18	(0.692) _{exp}
IBFM, Iachello et al. [31]	0.000	−0.280	(0.692) _{exp}
IBFM (quenched), Iachello et al. [31]	0.000	−0.168	(0.692) _{exp}
TFFS, Nikolaev–Klapdor-Kleingrothaus [32]		−0.186	—
SM (Bonn A), Ressel–Dean [27]	−0.009	−0.227	0.980 {0.637} _{eff}
QTDA, Engel [20]	−0.041	−0.236	0.70

The dimensionless integral $I(E_R)$ is dark-matter-particle velocity distribution correction

$$I(E_R) = \frac{\langle v^2 \rangle}{\langle v \rangle} \int_{x_{\min}} \frac{f(x)}{v} dx = \frac{\sqrt{\pi}}{2} \frac{3 + 2\eta^2}{\sqrt{\pi}(1 + 2\eta^2)\text{erf}(\eta) + 2\eta e^{-\eta^2}} [\text{erf}(x_{\min} + \eta) - \text{erf}(x_{\min} - \eta)],$$

where we assume that in our Galaxy rest-frame WIMPs have the Maxwell-Boltzmann velocity distribution and use the dimensionless Earth speed with respect

to the halo $\eta = 1$, $x_{\min}^2 = \frac{3}{4} \frac{M_A E_R}{\mu_A^2 \bar{v}^2}$. The error function is $\text{erf}(x) = \frac{2}{\sqrt{\pi}} \int_0^x dt e^{-t^2}$.

The velocity variable is the dispersion $\bar{v} \simeq 270$ km/s. The mean WIMP velocity $\langle v \rangle = \sqrt{\frac{5}{3}} \bar{v}$. We also assume both form-factors $F_{\text{SI,SD}}^2(E_R)$ in the simplest Gaussian form following Refs. [28, 29]. In particular, this allows rather simple equations (14) to be used, which are suitable for our consideration. Integrating the differential rate (1) from the recoil energy threshold ϵ to some maximal energy ϵ , one obtains the total detection rate $R(\epsilon, \epsilon)$ as a sum of the SD and SI terms:

$$R(\epsilon, \epsilon) = R_{\text{SI}}(\epsilon, \epsilon) + R_{\text{SD}}(\epsilon, \epsilon) = \int_{\epsilon}^{\epsilon} dE_R \kappa_{\text{SI}}(E_R, m_\chi) \sigma_{\text{SI}} + \int_{\epsilon}^{\epsilon} dE_R \kappa_{\text{SD}}(E_R, m_\chi) \sigma_{\text{SD}}. \quad (15)$$

To accurately estimate the event rate $R(\epsilon, \epsilon)$, one needs to know a number of quite uncertain astrophysical and nuclear structure parameters as well as the very specific characteristics of an experimental setup (see, for example, discussion in Refs. [35, 8]).

3. Nuclear spin structure at finite momentum transfer

As m_χ increases, the product qR starts to become non-negligible and the *finite momentum transfer limit* must be considered. With the isoscalar spin coupling constant $a_0 = a_n + a_p$ and the isovector spin coupling constant $a_1 = a_p - a_n$, one can split the nuclear structure function $S^A(q)$ into a pure isoscalar term, $S_{00}^A(q)$, a pure isovector term, $S_{11}^A(q)$, and an interference term, $S_{01}^A(q)$, in the following way

$$S^A(q) = a_0^2 S_{00}^A(q) + a_1^2 S_{11}^A(q) + a_0 a_1 S_{01}^A(q). \quad (16)$$

The relations $S_{00}^A(0) = C(J)(\langle \mathbf{S}_p \rangle + \langle \mathbf{S}_n \rangle)^2$, $S_{11}^A(0) = C(J)(\langle \mathbf{S}_p \rangle - \langle \mathbf{S}_n \rangle)^2$, and $S_{01}^A(0) = 2C(J)(\langle \mathbf{S}_p^2 \rangle - \langle \mathbf{S}_n^2 \rangle)$ with $C(J) = \frac{2J+1}{4\pi} \frac{J+1}{J}$, connect the nuclear spin structure function $S^A(q=0)$ with proton $\langle \mathbf{S}_p \rangle$ and neutron $\langle \mathbf{S}_n \rangle$ spin contributions averaged over the nucleus. These three partial structure functions $S_{ij}^A(q)$ allow calculation of spin-dependent cross sections for any heavy Majorana particle, as well as for the neutralino with arbitrary composition [26].

The calculations of the proton and neutron spins $\langle \mathbf{S}_{p(n)} \rangle$ averaged over all nucleons in the nucleus A , which are relevant to the zero-momentum neutralino-nucleon spin cross sections, are considered in Ref. [23]. All available sets of the spin structure functions are collected in [24] either in the form of explicit functions or as useful analytical parameterizations of the accurate numerical results. These functions describe recoil energy dependence of the differential event rate due to the spin-dependent neutralino-nucleon interaction, provided neutralino is a dark-matter particle. For the experimentally interesting nuclear systems ^{29}Si and ^{73}Ge , very elaborate calculations have been performed by Ressel et al. [22]. In the case of ^{73}Ge , a further improved calculation by Dimitrov, Engel and Pittel was carried out [33]. To perform modern data analysis in the finite momentum transfer approximation, it looks reasonable to use equations for the differential event rate (1) schematically given below

$$\begin{aligned} \frac{dR(\epsilon, \varepsilon)}{dE_R} &= \mathcal{N}(\epsilon, \varepsilon, E_R, m_\chi) \left[\eta_{\text{SI}}(E_R, m_\chi) \sigma_{\text{SI}}^p + \eta'_{\text{SD}}(E_R, m_\chi, \omega) a_0^2 \right], \quad (17) \\ \mathcal{N}(\epsilon, \varepsilon, E_R, m_\chi) &= \left[N_T \frac{c\rho_\chi}{2m_\chi} \frac{M_A}{\mu_p^2} \right] \frac{4\mu_A^2}{\langle q_{\text{max}}^2 \rangle} \left\langle \frac{v}{c} \right\rangle I(E_R) \theta(E_R - \epsilon) \theta(\varepsilon - E_R), \\ \eta_{\text{SI}}(E_R, m_\chi) &= \{ A^2 F_{\text{SI}}^2(E_R) \}, \\ \eta'_{\text{SD}}(E_R, m_\chi, \omega) &= \mu_p^2 \left\{ \frac{4}{2J+1} (S_{00}(q) + \omega^2 S_{11}(q) + \omega S_{01}(q)) \right\}. \end{aligned}$$

The isovector-to-isoscalar nucleon coupling ratio is $\omega = a_1/a_0$. Equations (17) allow experimental recoil spectra to be directly described in terms of only *three* [36] independent parameters (σ_{SI}^p , a_0^2 and ω) for any fixed WIMP mass m_χ (and any neutralino composition). Comparing this equation with the observed recoil spectra for different targets (Ge, Xe, F, NaI, etc) one can directly and simultaneously restrict both isoscalar and isovector neutralino-nucleon effective couplings $a_{0,1}$. These constraints will impose most model-independent restrictions on the MSSM parameter space.

3.1. Long-tail \mathbf{q} -behavior due to the spin

An attractive feature of the SD WIMP-nucleus interaction is the q -dependence of SD structure function (16). The ratio of SD to SI rate in the ^{73}Ge detector grows with the WIMP mass [37, 38]. The growth is much greater for heavy target isotopes like xenon. The reason is the different behavior of the spin and scalar structure functions with increasing momentum transfer. For example, the xenon SI structure function vanishes at recoil energy, but the SD xenon structure functions (Fig. 4) are still non-zero in the region. The structure functions completely determine the spin-dependent cross sections of elastic neutralino scattering off ^{131}Xe . As noted by Engel in Ref. [20], the relatively long tail of the SD structure function is caused by nucleons near the Fermi surface, which do the bulk of the scattering. The core nucleons, which dominate the SI nuclear coupling, contribute much less at large q . Therefore the SD efficiency for detection of a DM signal is higher than the SI efficiency,

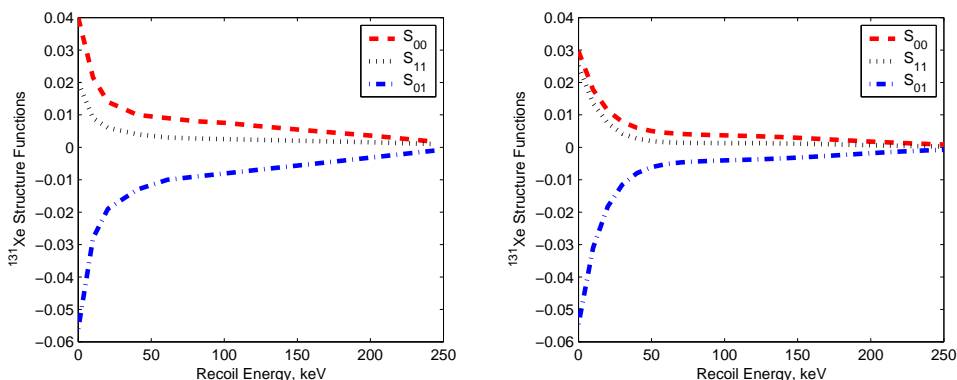


Fig. 4. Partial structure functions $S_{00}^{131}(q)$ (top), $S_{01}^{131}(q)$ (bottom) and $S_{11}^{131}(q)$ (middle) in ^{131}Xe as a function of the recoil energy. Left: results of Engel [20]. Right: the parameterizations of Ressel and Dean [27]. For ^{131}Xe , when the maximal WIMP velocity $v_{\max} = 600$ km/s, one has $q_{\max} \approx 487$ MeV/c and $E_{\max} \approx 963$ keV.

4. Cross sections in the effective low-energy MSSM

To estimate the expected direct DM detection rates (with equations (1), (15) or (17)) one should calculate cross sections σ_{SI} and σ_{SD} (or WIMP-nucleon couplings $a_{p,n}$) within the framework of some SUSY-based theory or take them from experimental data.

To obtain as much as general SUSY predictions, it appeared more convenient to work within a phenomenological SUSY model whose parameters are defined directly at the electroweak scale, relaxing completely constraints following from any unification assumption (see for example Refs. [39–41, 1, 42–44, 38, 37, 45, 12, 19, 18, 11]). This effective scheme of the MSSM is called the effMSSM in Ref. [46], and later the low-energy effective supersymmetric theory (LEEST) in Ref. [47, 48]. The effMSSM parameter space is determined by entries of the mass matrices of neutralinos, charginos, Higgs bosons, sleptons and squarks. In the MSSM, the lightest neutralino $\chi \equiv \tilde{\chi}_1^0$ is a mixture of four superpartners of gauge and Higgs bosons (Bino, Wino and two Higgsinos): $\chi = N_{11}\tilde{B}^0 + N_{12}\tilde{W}^0 + N_{13}\tilde{H}_1^0 + N_{14}\tilde{H}_2^0$. It is commonly accepted that χ is mostly gaugino-like if $P \equiv N_{11}^2 + N_{12}^2 > 0.9$ and Higgsino-like if $P < 0.1$, or mixed otherwise. The current experimental upper limits on sparticle and Higgs masses from the Particle Data Group [49] are included. Also the limits on the rare $b \rightarrow s\gamma$ decay [50, 51] following [52–55] have been imposed. For each point in the MSSM parameter space (MSSM model), the relic density of the light neutralino $\Omega_\chi h^2$ was evaluated with the code [43–45]. Two cosmologically interesting regions were considered. One is $0.1 < \Omega_\chi h^2 < 0.3$ and the other is the WMAP-inspired region $0.094 < \Omega_\chi h^2 < 0.129$ [4, 5]. A possibility for the LSP to be not a unique DM candidate with much smaller relic density $0.002 < \Omega h^2 < 0.1$ is also taken into account. Further details can be found in Ref. [10].

Typical WIMP-nucleon cross sections of both spin (SD) and scalar (SI) interactions as function of the WIMP mass are depicted as scatter plots in Figs. 5. One can see that the reduction of the allowed domain for the relic density does not significantly affect spin-dependent and the spin-independent WIMP-nucleon cross sections. The different behavior of these cross sections with mass of the LSP can be seen from the plots. There is a more stringent lower bound for the spin-dependent cross section. It is at a level of 10^{-7} pb. One can obtain the maximal values for the LSP-proton SD cross section in the pure Higgsino case (when only Z -exchange contributes) at a level of $5 \cdot 10^{-2}$ pb.

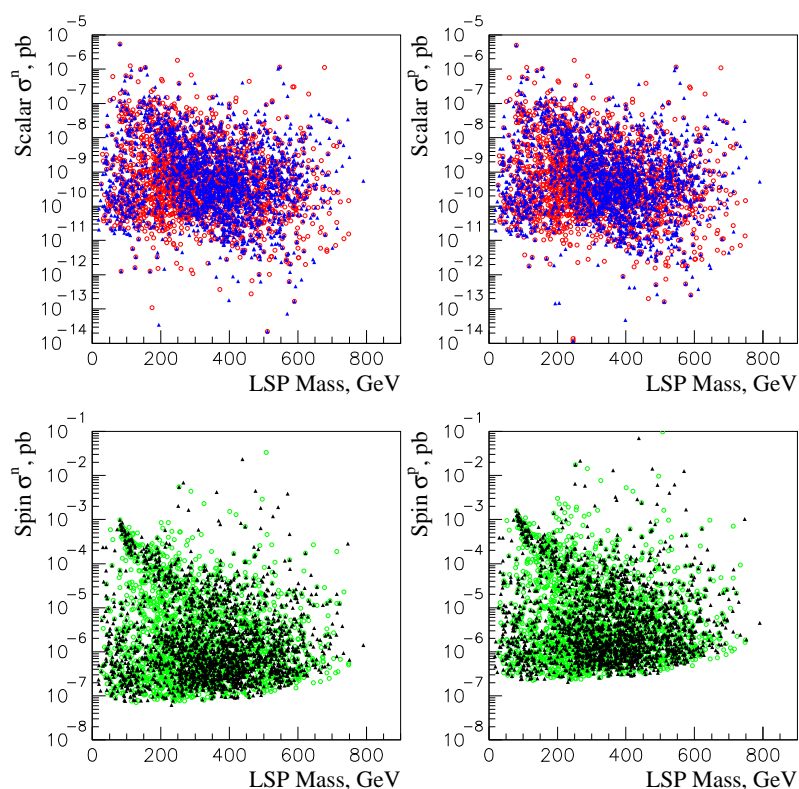


Fig. 5. Cross sections of spin-dependent and spin-independent interactions of WIMPs with proton and neutron. Filled triangles (light circles) correspond to relic neutralino density $0.1 < \Omega_\chi h^2 < 0.3$ ($0.025 < \Omega_\chi h^2 < 1$). From Refs. [37, 56, 43–45].

4.1. Do not miss a DM signal due to the spin

The difference in the SD and SI cross sections as well as the visible low bound for the SD cross sections indeed have important consequences for observations. The statement is illustrated in Fig. 6, where a comparison of the total spin-dependent

versus total spin-independent event rates in ^{73}Ge (with spin $J = 9/2$) is given. This isotope is one of the most promising high-spin isotopes for future construction of high-sensitivity detectors.

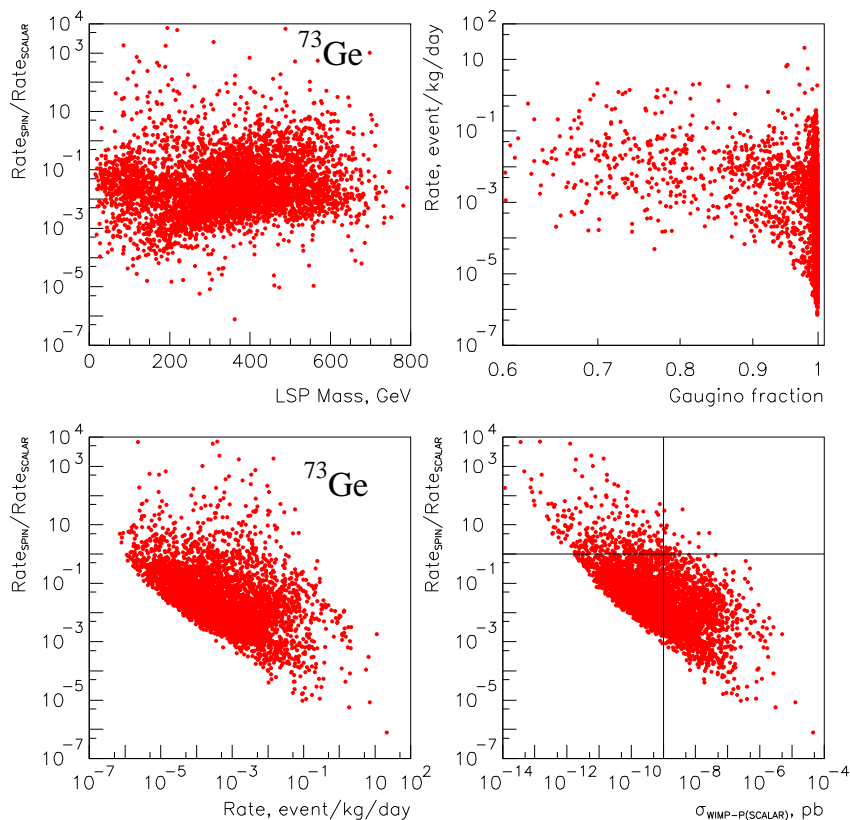


Fig. 6. Ratio of spin-dependent event rate to the spin-independent event rate in ^{73}Ge isotope as function of LSP mass (upper left), total (SD+SI) event rate (lower left) and scalar cross section of neutralino-proton interaction (lower right). The vertical line gives the best expected sensitivity of the GENIUS project [57–60]. In the region above the horizontal line, the spin contribution dominates. The total event rate versus gaugino fraction of LSP P is also given (upper right). From Ref. [37].

Figure 6 shows the weak increase of the ratio $R_{\text{SD}}/R_{\text{SI}}$ on mass of the LSP with the mean value being approximately 0.01–0.1. There are very large and very small values for the ratio practically for any mass of the LSP. The SI (or scalar) contribution obviously dominates in the domain of large expected rates in a Ge detector ($R > 0.1$ events/day/kg) as was obtained before (see, for example Ref. [11]). But as soon as the total rate drops down to $R < 0.01$ events/day/kg or, equivalently, the scalar neutralino-proton cross section becomes smaller than $10^{-9} \div 10^{-10}$ pb,

the spin-dependent interaction may produce a rather non-negligible contribution to the total event rate. Moreover, if the scalar cross section decreases further ($\sigma < 10^{-12}$ pb), it becomes obvious that the spin contribution alone saturates the total rate and protects it from decreasing below $R \approx 10^{-6} \div 10^{-7}$ events/day/kg [12]. This observation could be quite important for experiments actually looking for the direct *detection* of dark matter, not only for the exclusion plots. Therefore, if an experiment with sensitivity 10^{-5} – 10^{-6} event/day/kg fails to detect a dark matter signal, an experiment with a higher sensitivity should have a non-zero-spin target and will be able to detect dark matter particles only due to the spin neutralino-quark interaction.

4.2. Two constraints for SUSY due to the spin

From the general definitions of SD and SI WIMP-nucleus and WIMP-nucleon cross sections (Eqs. (3)–(7), (9) and (10)) one can conclude that the spin observables in DM search give us two independent constraints on a SUSY model via $\sigma_{SD}^p(0)$ and $\sigma_{SD}^n(0)$, or, equivalently, via a_p and a_n . These constraints are usually presented in the form of exclusion curves obtained with different target nuclei and recalculated in terms of $\sigma_{SD}^p(0)$ (see for example, Fig. 7) and $\sigma_{SD}^n(0)$ (see for example Fig. 8). This presentation is a bit obsolete [8, 25, 10], but it allows one to compare sensitivities of different experiments. At the current level of accuracy (when $f_q^{(p)} \approx f_q^{(n)}$ and $\sigma_{SI}^p(0) \approx \sigma_{SI}^n(0)$, see Fig. 5 there is only one similar constraint (given in Fig. 2) from spin-independent DM search experiments (see Eq. (3)).

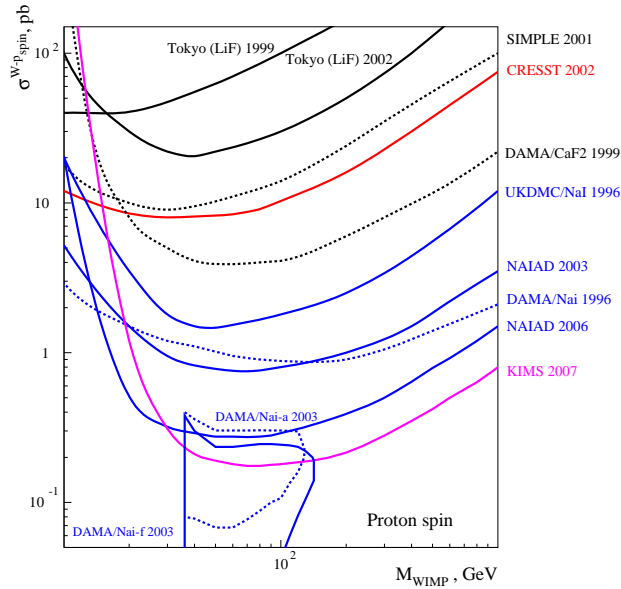


Fig. 7. Exclusion curves (2005) for the SD WIMP-proton cross section (σ_{SD}^p) versus WIMP mass). DAMA/NaI-7a(f) contours for WIMP-proton SD interaction in ^{127}I are obtained on the basis of annual signal modulation in the framework of a mixed scalar-spin coupling approach [8, 25]. From Ref. [10].

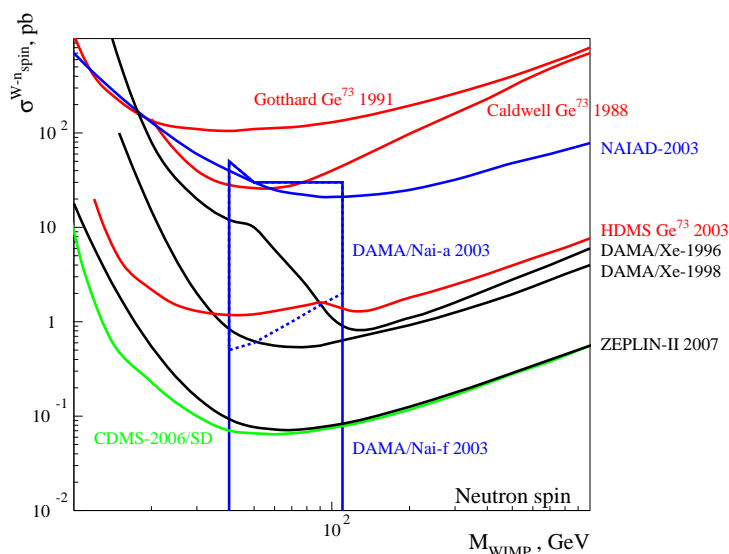


Fig. 8. Exclusion curves (2005) for the SD WIMP-neutron cross section (σ_{SD}^n versus WIMP mass). Note that the NAIAD curve here corresponds to the subdominant for ^{127}I WIMP-neutron SD interaction. The curve was extracted for the nucleus ^{127}I (which has a dominating WIMP-proton SD interaction) in the approach of Ref. [61]. It is much weaker in comparison with the relevant NAIAD curve for the WIMP-proton SD interaction in Fig. 7. From Ref. [10].

Indeed, for the spin-zero nuclear target the experimentally measured event rate (1) of direct DM particle detection, via Eq. (2) is connected with the zero-momentum WIMP-proton (neutron) cross section (3). The zero-momentum scalar WIMP-proton (neutron) cross section $\sigma_{\text{SI}}^p(0)$ can be expressed through effective neutralino-quark couplings \mathcal{C}_q (8) by means of expression (9). The couplings \mathcal{C}_q (as well as \mathcal{A}_q) can be directly connected with the fundamental parameters of a SUSY model such as $\tan\beta$, $M_{1,2}$, μ , masses of sfermions and Higgs bosons, etc. Therefore, experimental limitations on the SI neutralino-nucleon cross section supply us with a constraint on the fundamental parameters of an underlying SUSY model. In the case of the SD WIMP-nucleus interaction, from a measured differential rate (1) one first extracts a limitation for $\sigma_{\text{SD}}^A(0)$, and, therefore, has in principle two constraints [36] for the neutralino-proton a_p and neutralino-neutron a_n effective spin couplings, as follows from relation (4). From Eq. (4) one can also see that, contrary to the SI case (3), there is, generally, no factorization of the nuclear structure for $\sigma_{\text{SD}}^A(0)$. Both proton $\langle \mathbf{S}_p^A \rangle$ and neutron $\langle \mathbf{S}_n^A \rangle$ spin contributions simultaneously enter into Eq. (4) for the SD WIMP-nucleus cross section $\sigma_{\text{SD}}^A(0)$.

In the earlier considerations based on the OGM [30, 21], one assumed that the nuclear spin is carried by the “odd” unpaired group of protons or neutrons and only one of either $\langle \mathbf{S}_n^A \rangle$ or $\langle \mathbf{S}_p^A \rangle$ is non-zero. In this case, all possible target nuclei

can naturally be classified into neutron-odd and proton-odd groups. Following this classification, the experimental situation (in 2005) in the form of the exclusion curves for the SD WIMP-**proton** cross sections is given in Fig. 7. Although the DAMA/NaI-7 (2003) contours [8] are obtained on the basis of the annual signal modulation (closed contour), as well as in the mixed coupling framework (open contour) [25], the contours for the WIMP-proton SD interaction are also presented in the figure. The exclusion curves for the SD WIMP-**neutron** cross sections (in 2005) is given in Fig. 8. As in Fig. 7, the DAMA/NaI-7 (2003) [8] contours for the WIMP-neutron SD interaction (sub-dominant in ^{127}I) are placed in the figure. After 2005, new exclusion curves for the SD cross section from the CDMS [62] and EDELWEISS [63] experiments, with natural germanium bolometric detectors, became available. For comparison, Figs. 7 and 8 also show scatter plots for SD proton and neutron cross sections obtained in Ref. [10].

It is worth noting that the calculated scatter plots for σ_{SD}^p (Fig. 7) are obtained without any assumption about $\sigma_{\text{SD}}^n = 0$, but the experimental exclusion curves for σ_{SD}^p were traditionally extracted from the data ignoring fully the spin-neutron contribution, i.e. under the assumption $\sigma_{\text{SD}}^n = 0$. This *one-spin-coupling dominance scheme* (always used before a new approach was proposed in Ref. [61]) gave a bit too pessimistic exclusion curves, but allowed on the same ground the direct comparison of exclusion curves from different nuclear target experiments. Following Refs. [61] and [7–9], one obtains more stringent constraints on σ_{SD}^p assuming both $\sigma_{\text{SD}}^p \neq 0$ and $\sigma_{\text{SD}}^n \neq 0$, although usually for the proton-odd-like nuclei the contribution of the neutron spin is very small ($\langle \mathbf{S}_n^A \rangle \ll \langle \mathbf{S}_p^A \rangle$). Therefore, a direct comparison of the old-fashioned exclusion curves with the new ones is *generally* misleading. The same conclusion concerns [8, 9] direct comparison of the SI exclusion curves (obtained without any SD contribution) with the new SI exclusion curves (obtained with non-zero SD contribution), as well as with the results of the SUSY calculations (Fig. 2).

5. Conclusion

There is a continuous theoretical and experimental interest in existence of the cold dark matter in the Universe in the form of the weakly interacting massive particles (WIMPs). One of the best motivated non-baryonic WIMP dark matter candidates is the neutralino, the lightest supersymmetric particle. The motivation for supersymmetry arises naturally in modern theories of particle physics. To estimate the expected direct detection rate for these WIMPs, an effective low-energy minimal supersymmetric extension of the Standard Model (effMSSM) is used. There are some reasons to think that spin-dependent interaction of the DM WIMPs with nuclei could be very important. First, contrary to the only one constraint for SUSY models available from the SI WIMP-nucleus interaction, the SD WIMP-nucleus interaction supplies us with two such constraints. Second, for heavy target nuclei and heavy WIMP masses, the SD efficiency to detect a DM signal is much higher than the SI efficiency. Third, the absolute lower bound for the DM detection rate can naturally be due to SD interaction. An experiment aimed at *detecting* DM with

a sensitivity higher than 10^{-5} event/day/kg should have a non-zero-spin target.

We noted a possible incorrectness in the direct comparison of the exclusion curves for WIMP-proton (neutron) spin-dependent cross section obtained with and without non-zero WIMP-neutron (proton) spin-dependent contribution. This incorrectness concerns also the direct comparison of spin-dependent exclusion curves obtained with and without non-zero spin-independent contributions [8, 9]. To be consistent, for this comparison one has to use a mixed spin-scalar coupling approach. Finally, it is clear that without proper knowledge of the nuclear and nucleon structure it is not possible to extract reliably any useful information from very accurate direct dark matter search experiments.

Acknowledgements

This work was supported by JINR–Slovak Republic program and the Russian Foundation for Basic Research (grant 06–02–04003). V. A. B. thanks organizers of the Hadron Structure 2007 conference for the hospitality and the opportunity to present the above results.

References

- [1] L. Bergstrom, Rept. Prog. Phys. **63** (2000) 793; hep-ph/0002126.
- [2] P. de Bernardis et al., Nature **404** (2000) 955; astro-ph/0004404.
- [3] A. Balbi et al., Astrophys. J. **545** (2000) L1; astro-ph/0005124.
- [4] D. N. Spergel et al., Astrophys. J. Suppl. **148** (2003) 175; astro-ph/0302209.
- [5] C. L. Bennett et al., Astrophys. J. Suppl. **148** (2003) 1; astro-ph/0302207.
- [6] R. Massey et al., Nature **445** (2007) 286; astro-ph/0701594.
- [7] R. Bernabei et al., Phys. Lett. B **480** (2000) 23.
- [8] R. Bernabei et al., Riv. Nuovo Cim. **26** (2003) 1; astro-ph/0307403.
- [9] R. Bernabei et al., astro-ph/0311046.
- [10] V. A. Bednyakov and H. V. Klapdor-Kleingrothaus, Phys. Rev. D **70** (2004) 096006; hep-ph/0404102.
- [11] V. A. Bednyakov, H. V. Klapdor-Kleingrothaus and S. Kovalenko, Phys. Rev. **D50** (1994) 7128; hep-ph/9401262.
- [12] V. A. Bednyakov and H. V. Klapdor-Kleingrothaus, Phys. Rev. D **62** (2000) 043524; hep-ph/9908427.
- [13] G. Jungman, M. Kamionkowski, and K. Griest, Phys. Rept. **267** (1996) 195; hep-ph/9506380.
- [14] J. D. Lewin and P. F. Smith, Astropart. Phys. **6** (1996) 87.
- [15] P. F. Smith and J. D. Lewin, Phys. Rept. **187** (1990) 203.
- [16] V. A. Bednyakov and H. V. Klapdor-Kleingrothaus, Phys. Atom. Nucl. **62** (1999) 966.
- [17] V. A. Bednyakov, S. G. Kovalenko and H. V. Klapdor-Kleingrothaus, Phys. Atom. Nucl. **59** (1996) 1718.

- [18] V. A. Bednyakov, H. V. Klapdor-Kleingrothaus and S. G. Kovalenko, *Phys. Rev.* **D55** (1997) 503; hep-ph/9608241.
- [19] V. A. Bednyakov, S. G. Kovalenko, H. V. Klapdor-Kleingrothaus and Y. Ramachers, *Z. Phys. A* **357** (1997) 339; hep-ph/9606261.
- [20] J. Engel, *Phys. Lett. B* **264** (1991) 114.
- [21] J. Engel, S. Pittel and P. Vogel, *Int. J. Mod. Phys.* **E1** (1992) 1.
- [22] M. T. Ressell et al., *Phys. Rev. D* **48** (1993) 5519.
- [23] V. A. Bednyakov and F. Simkovic, *Phys. Part. Nucl.* **36** (2005) 131; hep-ph/0406218.
- [24] V. A. Bednyakov and F. Simkovic, *Phys. Part. Nucl.* **37** (2006) S106; hep-ph/0608097.
- [25] R. Bernabei et al., *Phys. Lett. B* **509** (2001) 197.
- [26] J. Engel, M. T. Ressell, I. S. Towner and W. E. Ormand, *Phys. Rev. C* **52** (1995) 2216; hep-ph/9504322.
- [27] M. T. Ressell and D. J. Dean, *Phys. Rev. C* **56** (1997) 535; hep-ph/9702290.
- [28] J. R. Ellis and R. A. Flores, *Nucl. Phys. B* **307** (1988) 883.
- [29] J. R. Ellis and R. A. Flores, *Phys. Lett. B* **263** (1991) 259.
- [30] J. Engel and P. Vogel, *Phys. Rev. D* **40** (1989) 3132.
- [31] F. Iachello, L. M. Krauss and G. Maino, *Phys. Lett.* **B254** (1991) 220.
- [32] M. A. Nikolaev and H. V. Klapdor-Kleingrothaus, *Z. Phys. A* **345** (1993) 373.
- [33] V. Dimitrov, J. Engel and S. Pittel, *Phys. Rev. D* **51** (1995) 291; hep-ph/9408246.
- [34] J. R. Ellis and R. A. Flores, *Nucl. Phys. B* **400** (1993) 25.
- [35] R. Bernabei et al., astro-ph/0305542.
- [36] V. A. Bednyakov, H. V. Klapdor-Kleingrothaus and S. G. Kovalenko, *Phys. Lett. B* **329** (1994) 5; hep-ph/9401271.
- [37] V. A. Bednyakov and H. V. Klapdor-Kleingrothaus, *Phys. Rev. D* **63** (2001) 095005; hep-ph/0011233.
- [38] V. A. Bednyakov, *Phys. Atom. Nucl.* **66** (2003) 490; hep-ph/0201046.
- [39] V. Mandic, A. Pierce, P. Gondolo and H. Murayama, hep-ph/0008022.
- [40] L. Bergstrom and P. Gondolo, *Astropart. Phys.* **5** (1996) 263; hep-ph/9510252.
- [41] P. Gondolo, hep-ph/0005171.
- [42] V. A. Bednyakov, *Phys. Atom. Nucl.* **67** (2004) 1931; hep-ph/0310041.
- [43] V. A. Bednyakov, H. V. Klapdor-Kleingrothaus and V. Gronewold, *Phys. Rev. D* **66** (2002) 115005; hep-ph/0208178.
- [44] V. A. Bednyakov, H. V. Klapdor-Kleingrothaus and E. Zaiti, *Phys. Rev. D* **66** (2002) 015010; hep-ph/0203108.
- [45] V. A. Bednyakov, hep-ph/0208172.
- [46] A. Bottino, F. Donato, N. Fornengo and S. Scopel, *Phys. Rev. D* **63** (2001) 125003; hep-ph/0010203.
- [47] J. R. Ellis, K. A. Olive, Y. Santoso and V. C. Spanos, *Phys. Rev. D* **69** (2004) 015005; hep-ph/0308075.
- [48] J. R. Ellis, A. Ferstl, K. A. Olive and Y. Santoso, *Phys. Rev. D* **67** (2003) 123502; hep-ph/0302032.

- [49] K. Hagiwara et al., Phys. Rev. D **66** (2002) 010001.
- [50] M. S. Alam et al., Phys. Rev. Lett. **74** (1995) 2885.
- [51] K. Abe et al., hep-ex/0107065.
- [52] S. Bertolini, F. Borzumati, A. Masiero and G. Ridolfi, Nucl. Phys. B **353** (1991) 591.
- [53] R. Barbieri and G. F. Giudice, Phys. Lett. B **309** (1993) 86; hep-ph/9303270.
- [54] A. J. Buras, M. Misiak, M. Munz and S. Pokorski, Nucl. Phys. B **424** (1994) 374; hep-ph/9311345.
- [55] A. Ali and C. Greub, Z. Phys. C **60** (1993) 433.
- [56] V. A. Bednyakov, H. V. Klapdor-Kleingrothaus and H. Tu, Phys. Rev. D **64** (2001) 075004; hep-ph/0101223.
- [57] H. V. Klapdor-Kleingrothaus, Nucl. Phys. Proc. Suppl. **110** (2002) 364; hep-ph/0206249.
- [58] H. V. Klapdor-Kleingrothaus et al., hep-ph/9910205.
- [59] J. Hellmig and H. V. Klapdor-Kleingrothaus, Z. Phys. A **359** (1997) 351; nucl-ex/9801004.
- [60] H. V. Klapdor-Kleingrothaus and M. Hirsch, Z. Phys. A **359** (1997) 361.
- [61] D. R. Tovey, R. J. Gaitskell, P. Gondolo, Y. Ramachers and L. Roszkowski, Phys. Lett. B **488** (2000) 17; hep-ph/0005041.
- [62] D. S. Akerib et al., Phys. Rev. D **68** (2003) 082002; hep-ex/0306001.
- [63] A. Benoit et al., Phys. Lett. B **545** (2002) 43; astro-ph/0206271.

VAŽNOST NUKLEARNOG SPINA ZA OPAŽANJE TAMNE TVARI

Masivne čestice sa slabim međudjelovanjem (WIMP-ovi) su među glavnim kandidatima za objašnjenje zaostatne tamne tvari (DM). Zamisao izravne detekcije DM zasniva se na spinski-ovisnom (SD) i spinski-neovisnom (SI) međudjelovanju WIMP-ova s jezgrama u meti. U ovom radu ističe se važnost SD međudjelovanja WIMP-jezgra za pouzdano opažanje DM. Primijenili smo efektivni niskoenergijski supersimetrični standardni model za računanje udarnih presjeka DM, uz pretpostavku da je neutralino najlakši WIMP. Pokazujemo da međudjelovanje SD WIMP-jezgra daje apsolutnu donju granicu za izravno opažanje tamne tvari, te preporučamo mjerenja s novom izvedbom, s osjetljivošću većom od 10^{-5} event/day/kg, koja bi trebala imati metu spina razlicitog od nule, kako bi se izbjeglo neopažanje DM signala.